Original Article

JCBFM

Journal of Cerebral Blood Flow & Metabolism
2017, Vol. 37(4) 1517–1526

DOI: 10.1177/0271678X16657574
journals.sagepub.com/home/jcbfm
SAGE

Is ultrasound perfusion imaging capable of detecting mismatch? A proof-of-concept study in acute stroke patients

Raluca Reitmeir[1,*], Jens Eyding[2,*], Markus F Oertel[1], Roland Wiest[3], Jan Gralla[3], Urs Fischer[4], Pierre-Yves Giquel[5], Stefan Weber[5], Andreas Raabe[1], Heinrich P Mattle[4], Werner J Z'Graggen[1] and Jürgen Beck[1]

Abstract

In this study, we compared contrast-enhanced ultrasound perfusion imaging with magnetic resonance perfusion-weighted imaging or perfusion computed tomography for detecting normo-, hypo-, and nonperfused brain areas in acute middle cerebral artery stroke. We performed high mechanical index contrast-enhanced ultrasound perfusion imaging in 30 patients. Time-to-peak intensity of 10 ischemic regions of interests was compared to four standardized nonischemic regions of interests of the same patient. A time-to-peak >3 s (ultrasound perfusion imaging) or >4 s (perfusion computed tomography and magnetic resonance perfusion) defined hypoperfusion. In 16 patients, 98 of 160 ultrasound perfusion imaging regions of interests of the ischemic hemisphere were classified as normal, and 52 as hypoperfused or nonperfused. Ten regions of interests were excluded due to artifacts. There was a significant correlation of the ultrasound perfusion imaging and magnetic resonance perfusion or perfusion computed tomography (Pearson's chi-squared test 79.119, $p < 0.001$) (OR 0.1065, 95% CI 0.06–0.18). No perfusion in ultrasound perfusion imaging (18 regions of interests) correlated highly with diffusion restriction on magnetic resonance imaging (Pearson's chi-squared test 42.307, $p < 0.001$). Analysis of receiver operating characteristics proved a high sensitivity of ultrasound perfusion imaging in the diagnosis of hypoperfused area under the curve, (AUC = 0.917; $p < 0.001$) and nonperfused (AUC = 0.830; $p < 0.001$) tissue in comparison with perfusion computed tomography and magnetic resonance perfusion. We present a proof of concept in determining normo-, hypo-, and nonperfused tissue in acute stroke by advanced contrast-enhanced ultrasound perfusion imaging.

Keywords

Acute ischemic stroke, cerebral perfusion, ultrasound perfusion imaging, brain imaging, neurosonology

Received 9 January 2016; Revised 14 April 2016; Accepted 17 May 2016

Introduction

Several studies have shown the potential of contrast-enhanced ultrasound for the discrimination of ischemic versus normally perfused brain tissue.[1–6] Ultrasound is noninvasive and can, unlike magnetic resonance imaging (MRI) or computed tomography (CT), be performed at the bedside.

Cerebral ultrasound perfusion imaging (UPI) can be used to differentiate ischemic and nonischemic lesions,[2] but it has not yet been investigated and compared to the gold standard for assessing brain tissue perfusion in patients with acute stroke, i.e. perfusion CT (CTP) or MR perfusion imaging (MRP).

[1]Department of Neurosurgery, Inselspital, Bern University Hospital, University of Bern, Bern, Switzerland
[2]Department of Neurology, University Hospital, Knappschaftskrankenhaus, Ruhr University Bochum, Bochum, Germany
[3]Institute of Diagnostic and Interventional Neuroradiology, Inselspital, Bern University Hospital, University of Bern, Bern, Switzerland
[4]Department of Neurology, Inselspital, Bern University Hospital, University of Bern, Bern, Switzerland
[5]ARTORG Center for Biomedical Engineering, University of Bern, Switzerland

*These authors contributed equally to this work.

Corresponding author:
Jens Eyding, Department of Neurology, University Hospital Knappschaftskrankenhaus, Ruhr University Bochum, Bochum, Germany.
Email: eyding@web.de

In UPI, two basic techniques are used to display parenchymal microvascular blood supply: the bolus-kinetic approach and the refill-kinetic approach.[7] The bolus-kinetic approach analyzes time–intensity curves after a bolus injection of a fixed dose of contrast enhancer.[8] The refill-kinetic approach analyzes noise alterations when the blood concentration of contrast enhancer reaches steady state. In steady state, high mechanical index (HighMI) energy is applied to destroy the microbubbles that serve as contrast enhancer, and then the refilling characteristics of the contrast enhancer can be evaluated.[9] Both approaches have been examined in stroke patients and in patients with cerebral neoplasms. In stroke patients, ischemic areas can be demonstrated.[2,3,6,10] Both techniques, the HighMI bolus-kinetic approach and the refill-kinetic approach have been used to differentiate critically hypoperfused (penumbra) and irreversibly ischemic areas (infarct core).[2,3] However, the HighMI bolus-kinetic technique was not compared to MRP or CTP and the refill-kinetic approach showed poor specificity.[2,3]

The aim of this study was to analyze the diagnostic accuracy of UPI to assess cerebral parenchymal perfusion in acute ischemic stroke and compare it with MRP or CTP. The study was performed in a selected group of patients with acute ischemic stroke who all were investigated with MRP or CTP and immediately thereafter underwent endovascular therapy.

Subjects and methods

Patients

Patients with an acute middle cerebral artery (MCA) stroke admitted to the Neurocenter of the University Hospital Bern between October 2012 and March 2014 were evaluated for thrombolysis according to the Bernese neurologic stroke algorithm.[12] If a patient qualified for interventional therapy or thrombolysis and an experienced sonographer (JE, RR, MO) was available, the patient was enrolled in this study after stroke CT or MRI with perfusion imaging had been performed. Exclusion criteria were insufficient bone window when standard landmarks could not be depicted, age below 18 years, or severe heart and lung disease which were contraindications to the echo-contrast agent Sonovue (Bracco, Milan, Italy). The UPI investigation was performed in the angio-suite during preparations for endovascular therapy and did not delay the intervention procedure.

Clinical status was documented using the National Institute of Health Stroke Scale on admission.

The protocol for collecting data was in accordance with the 1996 revision (Somerset West, RSA) of the Declaration of Helsinki (1964) and was approved by the local ethics committee (Kantonale Ethikkommission Bern No. KEK 179/12).

Informed consent was obtained in a two-step procedure: in the acute phase of the study the patients' relatives and an independent physician approved the participation of the patient in the study and in the follow-up phase, up to three months after stroke, the patients themselves or their legal representatives approved study participation.

UPI

All examinations were performed using a Philips iU22 ultrasound machine (Philips Healthcare, Andover, MA, USA) equipped with a 1–5 MHz dynamic sector array (S5-1). Peak systolic velocities of both MCAs were determined first. The field of view was set to an imaging depth of 150 mm in a sector angle of 90°. Imaging plane was then tilted to the diencephalic plane as described before,[2] where the frontal horns of the side ventricles and the third ventricle serve as landmarks and where the contralateral MCA territory (insular cortex, subcortical white matter, and cortical gray matter of the parietal and temporal lobe, basal ganglia) can be visualized well without artifacts from major vessels.

HighMI UPI bolus imaging from the nonischemic side was performed as described previously.[10] Data acquisition of 45 s was started immediately after i.v. injection of a 2.0 ml bolus of the second-generation contrast enhancer SonoVue (Bracco International, Milano, Italy) followed by a 10 ml flush of saline using an MI setting of 1.34 and a frame rate of 5 Hz.

Postprocessing image data of UPI

UPI data were analyzed offline by three different investigators (JE, RR, MO). Two different approaches were applied: (1) using a dedicated algorithm[2] running on MatLab R2009b (Mathworks, Massachusetts, USA), fitting a bolus-model function and extracting specific parameters of perfusion and (2) using a commercially obtainable software (VueBox 4.3, Bracco Imaging, Geneva, Switzerland). With this combination of systems both region-wise analysis and analysis of calculated parameter images for the time-to-peak (TTP) intensity were performed. As an intraindividual reference value the median TTP value of the following four prespecified regions of interest (ROIs) of the nonaffected hemisphere of each patient was used: head of caudate nucleus, lentiform nucleus, anterior and posterior thalamus. The other 10 prespecified ROIs were in the following territories of the affected hemisphere: caudate nucleus, lentiform nucleus, anterior MCA white matter, middle MCA white matter, posterior MCA white matter, anterior MCA gray matter, middle MCA gray matter, posterior MCA gray

matter, or in the anterior and posterior thalamus (Figure 1(a) and (b)). Rectangle ROIs in UPIs were manually set with a size of approximately 7 mm × 7 mm in basal ganglia and thalamus and 10 mm × 20 mm in white matter and gray matter.

Tissue perfusion of the affected MCA territory was graded into three categories according to TTP values. The individual median values of the nonaffected contralateral ROIs served as reference. Cutoff thresholds of 3 and 4 s delay were used to evaluate which thresholds of delay served better to distinguish normal perfusion and hypoperfusion:[14]

1. Normal perfusion: TTP within ≤3 or ≤4 s.
2. Hypoperfusion: TTP delay of >3 or >4 s.
3. No perfusion: no rise in the time–intensity curve detectable.

Description of standard versus patient-adjusted quantification algorithm

CT/MRI perfusion data were analyzed by three different investigators (RW, MO, RR) using OleaSphere Medical Imaging Software (Version 2.3, Cambridge, MA, USA). The size of the ROIs was 50 mm^2 (head of caudate nucleus, lentiform nucleus, anterior and posterior thalamus) and 200 mm^2 (anterior MCA white matter, middle MCA white matter, posterior MCA white matter, anterior MCA gray matter, middle MCA gray matter, posterior MCA gray matter). Two different quantification algorithms, standard versus patient adjusted, were used.

For the first quantification algorithm (standard plane), the depicted ROIs were placed on a standard diencephalic plane as described previously,[1] i.e. all

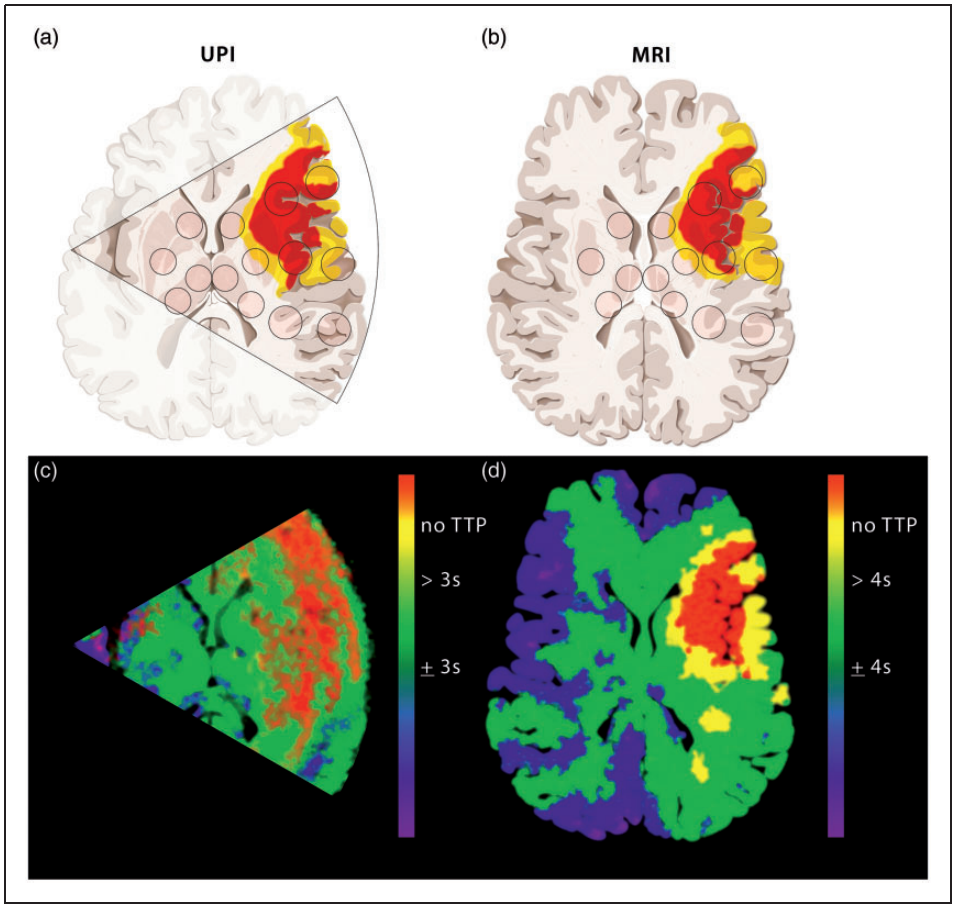

Figure 1. Overview of the perfusion categories of the regions of interest (ROIs) in the ischemic hemisphere as measured by CTP/MRP and/or UPI. Schematic representation of the different diagnostic levels comparing the UPI insonation level (a) and the MRI scanning level (b) in a patient with left MCA occlusion. Sectional schematic images from HighMI UPI of the contralateral side (a) and axial images from MRI with perfusion imaging (b). Parametric images from UPI (c) and MRP (d) with threshold representation as described in our study (UPI 3 s; MRP 4 s). According to the threshold representation of the normal perfused (green), hypoperfused (yellow) and nonperfused (red) tissue. (Copyright Neurosurgery Department, Inselspital, Bern, Switzerland).

ROIs are analyzed on the identical axial plane for both hemispheres. In order to compare the two investigational procedures, UPI versus CTP/MRP, we had to take into account the difference in anatomical regions: whereas CTP/MRP investigations were always done in a strictly axial plane (Figure 2(a)), the insonation plane for the UPI investigation was inclined 10–20° from the standard axial plane (Figure 2(b)). With UPI, different anatomical structures are analyzed for the two hemispheres because ROI location is higher on the contralateral side then its correlate on the CTP/MRP.

Therefore, we introduced a second quantification algorithm (patient adjusted), in which we used an upper and a lower diencephalic plane in the CTP/MRP investigation. We defined the upper diencephalic plane by identification of lateral ventricles with their anterior and posterior horns, the plane crossing the third ventricle in its upper region surrounded by the thalamic and basal ganglia structures. The lower level was defined by its relation to the third ventricle, which is crossed tangentially, and includes deeper thalamic and basal ganglia nuclei. These two planes were individually adjusted according to the anatomical landmarks on the parametric representation of the UPI investigation (Figure 1(c)). The respective upper or lower plane was selected and correlated to the parametric images of the UPI investigation as calculated by the respective software in order to best possible correlate the CT/MRI slices with the insonation level (Figure 2). The placement of the ROIs was performed after consensus of at least two of the three investigators (RW, MO, RR).

TTP measurements of the ROIs on MRIs and CTs were classified similarly as the ROIs of the UPI investigation. The individual median of nonaffected contralateral ROIs served as reference and the cutoff threshold used was a delay of 4 s.[11,13]

1. Normal perfusion: TTP within ≤4 s.
2. Hypoperfusion: TTP delay of >4 s.
3. No perfusion: no rise in the time–intensity curve detectable.

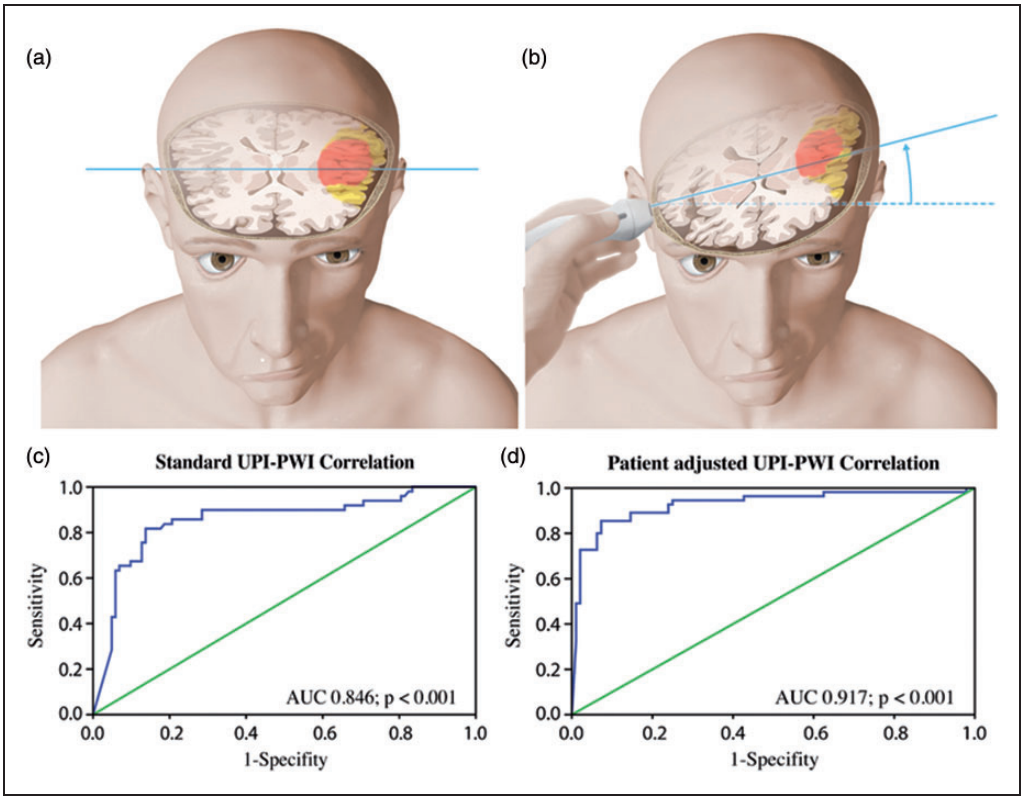

Figure 2. Schematic representation of the different diagnostic levels showing the MRI scanning level (a) and the UPI insonation level (b) in a patient suffering of left middle cerebral artery occlusion. Representation of the diencephalic insonation level through the third ventricle and visualization of ipsi- and contralateral basal ganglia. Note that the insonation level has a 10–20° inclination in comparison to the MRI scanning level, causing anatomical differences between the two hemispheres. (c, d) ROC curves of UPI in comparison with MRP. Using the patient-adjusted analysis algorithm (b) the specificity of the UPI investigation increased in comparison to the standard analysis algorithm (a). (Copyright Neurosurgery Department, Inselspital, Bern, Switzerland.

Statistical evaluation

The data were analyzed by descriptive statistics using the mean, median, and standard deviation (SD) of the ROIs. Sensitivity and specificity analyses were calculated using Pearson's chi-square test with a p-value < 0.05 considered significant. Odds Ratio and 95% CI were estimated.

In order to select the cutoff threshold, which according to the literature may be between 3 and 4 s,[5,10] receiver-operator characteristic (ROC) curves were used to obtain diagnostic threshold values of perfusion and diffusion parameters. These curves were made for the TTP delay values of UPI and perfusion MRI/CT on one side and for the TTP delay values of UPI and diffusion MRI on other side. An area under the curve of > 0.80 was considered to be a good test, of > 0.90 was considered to be an excellent test. From the ROC curve, we derived the optimal threshold value to estimate the TTP delay in UPI which best determines the perfusion and diffusion deficit in comparison with the CTP/MRI TTP values. Pearson correlation was used to evaluate correlations between absolute values of UPI TTP and MRI TTP values.

Statistical calculations were done using the SPSS Statistics Software (Version 22, Chicago, IL, USA).

Availability of data and materials. All the materials, data, and associated protocols will be available to the referees at submission and to the readers by request.

Results

Thirty patients were eligible according to the inclusion criteria; the mean (±SD) age was 75.5 ± 9.25 years. All patients tolerated the contrast-enhanced UPI investigation well without side effects.

Four patients (13.3%) had to be excluded because of insufficient temporal bone window, two (6.7%) because of inadequate quality of the MRP, six (20%) because of motion artifacts during the UPI investigation, and two (6.7%) because of previously unknown low cardiac output with insufficient rise of the time–intensity curve. The remaining 16 patients were included for further analysis. The clinical baseline data are displayed in Table 1. The general characteristics of the group of patients are presented in Table 2.

All patients underwent digital subtraction angiography that proved vessel occlusion and received mechanical recanalization no later than 6 h after onset of symptoms (mean 4.4 h, SD 1.73 h); seven patients received i.v. bridging lysis and thrombectomy, seven patients received only thrombectomy, and two patients were intravenously thrombolyzed.

Altogether, perfusion imaging was performed in 16 patients, in two with CT and 14 with MRI.

Table 1. Baseline data of 16 patients selected according to study criteria for UPI investigation before intraarterial thrombolysis.

Age in years, mean (SD)	76.5 (5.4)
Female, %	56
Baseline NIHSS score, mean (SD)	7.5 (6.3)
Occlusion localization	
Internal carotid artery, n (%)	3 (18.75)
Carotid-T, n (%)	3 (18.75)
MCA M1, n (%)	6 (37.5)
MCA M2, n (%)	2 (12.5)
MCA M3/4, n (%)	2 (12.5)
Patients receiving intravenous lysis, n (%)	11 (68.75)
SOT to intravenous lysis in hours, mean (SD)	2.58 (0.75)
SOT to MRI in hours, mean (SD)	2.23 (1.15)
SOT to UPI in hours, mean (SD)	3.31 (1.18)
SOT to cerebral angiography in hours, mean (SD)	4.25 (1.8)
SOT to intraarterial lysis/thrombectomy in hours, mean (SD)	4.40 (1.73)

MCA: middle cerebral artery; MRI: magnetic resonance imaging; NIHSS: National Institutes of Health Stroke Scale; SD: standard deviation; SOT: symptom onset time; UPI: ultrasound perfusion imaging.

A total of 320 ROIs were investigated in the ischemic hemisphere in CT/MRI and in the UPI investigation (160 ROIs for standard level and 160 ROIs for the patient-adjusted level quantification method). TTP measurement was feasible in all ROIs of the CT/MRI investigations, whereas for 10 ROIs in the UPI Investigation no TTP measurement was possible because of motion/insonation artifacts (four ROIs of contralateral anterior thalamus, three ROIs of contralateral anterior MCA white matter, and three ROIs of contralateral anterior MCA gray matter). There was no difference in the dropout rate in-between cortical and subcortical areas (three subcortical ROIs versus three cortical ROIs). Based on patient-adjusted analysis of perfusion, seven patients (70 ROIs) were analyzed at the lower diencephalic level and nine patients (90 ROIs) were analyzed at the higher diencephalic level. The mean TTP delay in the ischemic hemisphere in comparison to the nonischemic hemisphere was 4.7 ± 2.1 s for CTP and 3.72 ± 1.7 s for MRP (CTP and MRI combined was 3.82 ± 1.2 s).

Comparison of dedicated software and VueBox 4.3

Comparison of repeated analyses of TTP values in the corresponding ROIs did not show different values between the dedicated algorithm and Vuebox 4.3.

Table 2. Characteristics of studied patients.

Patient nr.	Age	Side	Diagnostic	NIHSS A	NIHSS FU	Most proximal occluded vessel	Therapy	Therapy success	Problems
1	76	Right	MRI	15	17	RACM1	Bridging lysis and thrombectomy	TICI2a	–
2	93	Right	CTP	17	3	RACM1	Bridging lysis	TICI2b	Cardiac failure
3	72	Left	MRI	6	13	LICA	Thrombectomy	TICI2b	–
4	81	Left	MRI	17	5	LICA	Thrombectomy	TICI3	–
5	90	Left	MRI	20	19	LACM1	Thrombectomy	TICI 2b	Insufficient BW
6	75	Right	MRI	8	0	RACM1	Thrombectomy	TICI2b	–
7	80	Right	CTP	4	3	RICA	Bridging lysis and thrombectomy	TICI1	–
8	70	Right	MRI	13	13	RICA	Thrombectomy	TICI1	–
9	86	Left	CTP	24	24	LACM1	Bridging lysis and thrombectomy	TICI2b TIMI 2	–
10	79	Right	CTP	17	9	RICA	Thrombectomy and intraarterial lysis	TICI3 TIMI3	Insufficient BW
11	81	Left	MRI	ITN	died	LACM1	Thrombectomy	died	Cardiac failure
12	78	Right	MRI	11	11	RACM1	Thrombectomy	TICI2b	–
13	65	Left	MRI	21	0	LICA-T	Thrombectomy	TICI2b	Artifacts UPI
14	70	Right	MRI	8	6	RACM2	ivL		Insufficient BW
15	85	Right	MRI	7	3	RACM1	Thrombectomy		–
16	80	Right	MRI	15	20	RACM1	Thrombectomy	TICI2a	Artifacts UPI
17	65	Left	MRI	3	2	LACM2	Bridging lysis and thrombectomy	TICI2b	–
18	63	Right	MRI	7	0	RACM1	Thrombectomy	TICI3	Artifacts UPI
19	49	Left	MRI	19	9	LICA-T	Thrombectomy	TICI3	Insufficient BW
20	80	Right	MRI	14	31	RICA	Thrombectomy	TICI2b	–
21	68	Left	MRI	11	11	LACM2	Thrombectomy	TICI2b	Artifacts UPI
22	56	Right	CTP	7	0	RACM1	Thrombectomy	TICI3	Artifacts UPI
23	75	Right	CTP	16	1	RMCA	ivL		Artifacts UPI
24	73	Left	MRI	15	3	LMCA	ivL		–
25	74	Right	MRI	5	0	RACM2	Bridging lysis and thrombectomy	TICI3	–
26	74	Right	MRI	25	19	RACM3	ivL		Artifacts MRI
27	80	Right	CTP	19		RICA	Bridging lysis and thrombectomy	TICI2b	Artifacts CT
28	76	Left	MRI	7	6	LACM4	ivL		–
29	74	Left	MRI	3	0	LMCA3	Bridging lysis and thrombectomy		–
30	71	Left	MRI	20	2	LMCA1	Bridging lysis and thrombectomy	TICI2b	–

Subjectively, the dedicated algorithm generated better parametric images (Figure 3) whereas the use of Vuebox for TTP quantification was easier to perform. Therefore, only the VueBox settings were used for further analyses. The parametric images generated by the dedicated algorithm were used to define the adequate MRI level for quantification of the patient-dependent algorithm.

Correlation with the gold standard

From the 160 ROIs investigated in the ischemic hemispheres and 64 ROIs in the nonischemic hemispheres, a total of 10 ROIs were excluded because of border- or stripe-field artifacts.[15] TTP measurement in the UPI was feasible in 132 ROIs. In 18 ROIs no TTP was measurable due to missing rise of the time–intensity

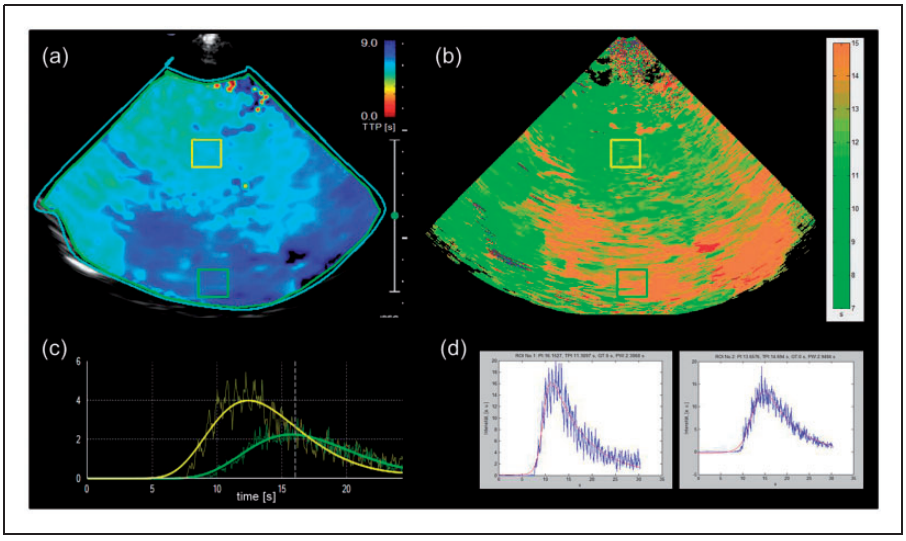

Figure 3. Comparison of TTP maps and ROI analysis between VueBox and dedicated software. Patient 7 with M1 occlusion of RMCA with imaging performed 278 min after symptom onset. (a) and (b). Screenshots of VueBox derived analysis with color-coded TTP map displaying both hemispheres with a marked area of delayed intensity rise in the RMCA territory (dark blue area a), exemplary time–intensity curves (TIC, c) derived from thalamic area of unaffected hemisphere (yellow box, TTP = 11.41 s), and from hypoperfused cortical area of affected hemisphere (green box, TTP = 14.70 s). (b) and (d). Corresponding color-coded TTP map (b) and example TICs (d) derived from thalamic area (yellow box, TTP = 11.31 s) and cortical area (green box, TTP = 14.69 s) by dedicated software.

curve (categorized as "no perfusion"). These ROIs were significantly correlated with the ROIs showing diffusion restriction on diffusion-weighted imaging (Pearson's chi-square coefficient 42.307; $P < 0.001$; Table 3). The coefficient of determination R^2 of 0.519 was measured by linear regression scatter plot analysis (Figure 4(c)). Comparison of ischemic versus nonischemic hemispheres showed a mean delay of TTP of 2.21 ± 1.3 s in ischemic tissue.

Selecting UPI-perfusion thresholds

In order to select the cutoff threshold, which according to the literature may be between 3 and 4 s,[5,10] we performed receiver-operator analysis to identify the best threshold for UPI as compared to the gold standard. A TTP delay value of 3 s was shown to be the threshold for defining hypoperfused ROIs in the UPI investigation (AUC = 0.917; $p < 0.001$).

ROC curve quantification was used to choose between the two quantification algorithms: standard versus patient adjusted. The measurements done by the standard level quantification algorithm showed good sensitivity of the predictive value for the UPI HighMI investigation in comparison with MRP sequences (AUC = 0.846; $p < 0.001$) but lower sensitivity than as compared to the patient-adjusted algorithm (AUC = 0.917; $p < 0.001$) (Figure 2(c) and (d)). Based on these results, further statistical analyses were done with TTP values originating from the patient-adjusted algorithm.

Table 3. Overview of the perfusion categories of the regions of interest (ROIs) in the ischemic hemisphere as measured by CTP/MRP and UPI.

Regions of interest	CTP/MRP (n)	UPI (n)	Pearson's chi-squared test	Statistical significance
Normal perfusion	101	98		
Hypoperfusion	31	34	79.119*	$p < 0.001$*
No perfusion	28	18	42.307	$p < 0.001$
Excluded ROIs	0	10		
Total	160	160		

*Normal perfusion versus hypoperfusion. CTP: perfusion computed tomography; MRP: magnetic resonance perfusion; UPI: ultrasound perfusion imaging.

The diagnostic predictive value of the HighMI UPI in comparison with the diagnostic MRI, using patient-adjusted ROC analysis, showed a high sensitivity and specificity of the UPI both in discriminating hypoperfused tissue (AUC = 0.917; $p < 0.001$) and nonperfused tissue (AUC = 0.830; $p < 0.001$) from normal tissue (Figure 4).

HighMI UPI showed sensitivity and specificity of 88.6 and 94.8%, respectively, with a positive predictive

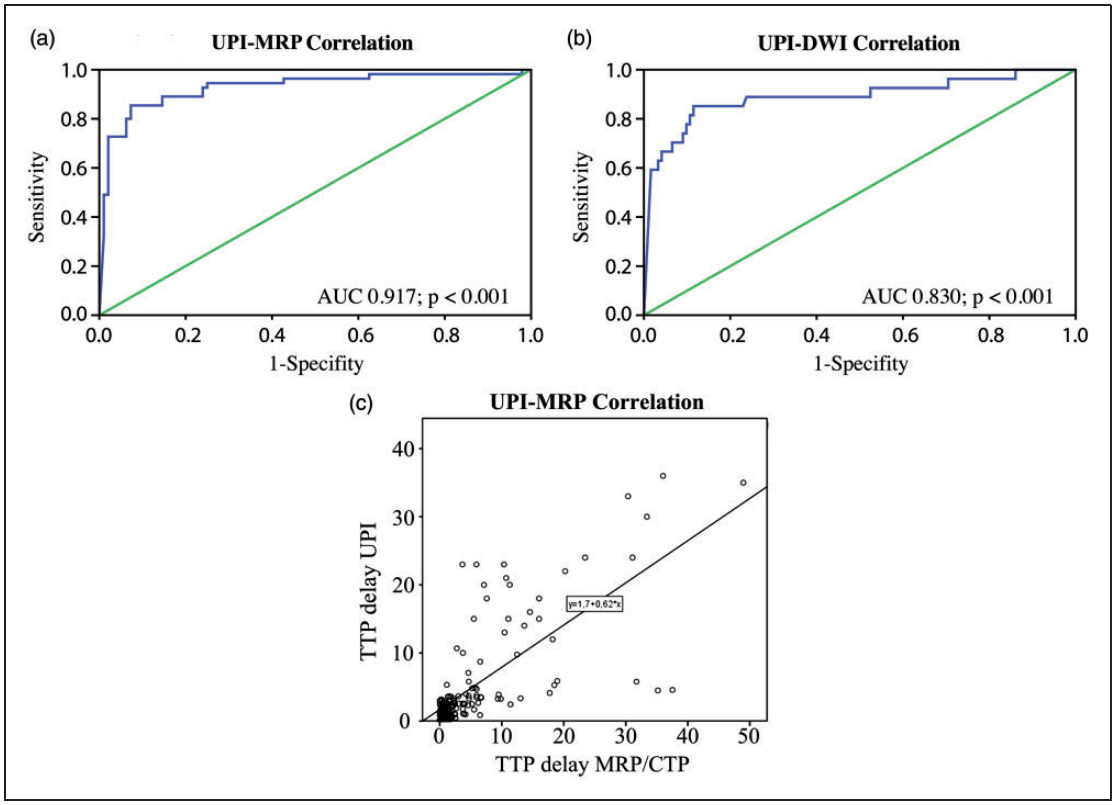

Figure 4. Comparison of UPI-based quantification of hypoperfused and nonperfused area with the gold standard-based quantification for hypoperfusion CTP/MRP and nonperfusion DWI. Receiver operating characteristics (ROC) curves of UPI in comparison with MRP and DWI. Detection of the hypoperfused tissue showed high sensitivity and specificity in comparison to CTP/MRP (a). The same was observed for detection of nonperfused tissue, where the nonperfused UPI ROIs were correlated with DWI regions on MRI (b). Scatter plot showing the linear correlation between absolute TTP delay values measured by UPI versus perfusion CT/MRI. R^2 Coefficient of determination is 0.519 (c).

value of 90.38% and negative predictive value of 93.81% in comparison with CTP/MRP of the diagnostic imaging. Pearson's correlation coefficient was statistically significant for HighMI UPI and perfusion-weighted sequences of the diagnostic MRI ($R = 0.558$; $p < 0.001$) (OR 0.1065, 95% CI 0.06–0.18).

Discussion

The current algorithm of HighMI UPI in acute MCA stroke provides high sensitivity and specificity to differentiate potentially reversible hypoperfusion (penumbra) and absent perfusion (infarct core) in comparison to the gold standard, perfusion-weighted MRI and CTP. Contrast enhanced UPI is noninvasive, repeatable, and portable and has been tested in subacute and chronic stroke and cerebral neoplasms.[2,3,6,10,14] Few attempts have been made to discriminate hypoperfused tissue in the penumbra from the nonperfused infarct core and from normal tissue in acute stroke. In this study we used HighMI UPI in acute stroke before endovascular therapy to assess cerebral perfusion semiquantitatively; the strength of the study is the comparison and validation of the results to the gold standards, MRP and CTP.

Another feature of this study is the use of HighMI UPI instead of LowMI UPI. Even though there has not yet been performed any direct comparison between the two methods, HighMI UPI may have the advantage of a direct comparison of perfusion parameters between the affected and the nonaffected hemisphere. The insonation depth of LowMI UPI is limited to the hemisphere ipsilateral to the ultrasound probe, while insonation of HighMI UPI reliably comprises both hemispheres, enabling the creation of an intraindividual normal value for comparison with the affected (i.e. "contralateral") hemisphere (so-called mirror approach). On the other hand, LowMI ultrasound has a lower spatial but probably a higher temporal resolution than High-MI ultrasound and may, furthermore, enable multiple measurements per examination.

In MRP a TTP delay greater than 4 s compared to the nonischemic hemisphere indicates reduced perfusion.[13] In UPI the cutoff threshold for identification

of impaired perfusion has been reported to be between 3 and 4 s.[10,14] Eyding et al. showed that a cutoff threshold of 4.04 s correlated best with the MRP delay.[10] The present study adjusted for the axial diencephalic plane of the MRP, with 20° upward inclined plane of the ultrasound probe. Multilevel ROI quantifications were done at the upper and lower diencephalic levels and the appropriate ROIs were selected for further analyses. Due to this allowance of a 20° shift the prognostic value of UPI increased from AUC = 0.846 to AUC = 0.917 (Figure 2).

Most studies published to date operated with dedicated software. We compared one of the latest commercially available quantification tools, VueBox 4.3, against the dedicated software for evaluation of hypoperfused tissue. Because the results of the ROI analyses were identical with VueBox, we decided to use only the VueBox analyses. As already underlined in ''Results'' section, the quantification of parametric images by dedicated software created more interpretable images than those generated by VueBox, so we suggest that color coding and the ability to adjust time limits should be improved in future quantification tools (Figure 3).

Our study has important limitations. We investigated a highly selected group of patients. Only patients selected for diagnostic cerebral angiography and endovascular therapy were included, and an additional prerequisite was the availability of a diagnostic perfusion CT or MRI of adequate quality. Of 30 screened patients, only datasets of 16 patients could be used to compare UPI to the gold standard CTP or MRP, so the external validity is limited. A total of 10 patients had to be excluded from UPI analyses due to restricted temporal bone window (n = 4) and movement artifacts (n = 6), highlighting the well-known fact that ultrasound examinations are examiner dependent. However, this study was designed as a proof of concept, so that the focus was rather on the potential of the method than on clinical applicability. Further investigations are surely needed to confirm our results in a clinical setting.

Some methodological limitations of the UPI are to be discussed. The single 2D imaging plane of the UPI compromises the measurement of hypoperfused and ischemic volume in comparison to CT or MR. Future development of 3D insonation systems may overcome this limitation. A stable angle of insonation could not be performed in six (20%) of patients because of patients' agitation and confusional state. Further development of the ultrasound brain helmet in humans may overcome this limitation in the future.[16]

The clinical application of UPI is and will probably remain at best complementary to CT/MR imaging, even if it proves useful for assessing cerebral perfusion in other pathological conditions such as subarachnoidal hemorrhage, tumor, brain death, trauma, or epilepsy. Nevertheless, UPI has the advantage of being a portable diagnostic tool; the idea of using ultrasound in a mobile stroke unit instead of a heavy CT scanner is appealing. Ultrasound could be used to exclude hemorrhage[17] and to prove hypoperfusion and thus ischemia in order to start intravenous thrombolysis on site. If exclusion of intracranial hemorrhage,[17] verification of intracranial vessel occlusion, and perfusion delay proves reliable, ultrasound may play a substantial role in future diagnosis of acute stroke and especially prehospital stroke management.

In conclusion, our study demonstrates that HighMI UPI in acute stroke is highly specific and sensitive for detecting hypoperfused and nonperfused areas. The results of UPI compared favorably with the gold standard CTP and MRP.

Funding

The author(s) disclosed receipt of the following financial support for the research, authorship, and/or publication of this article: The study was supported by grants of the Swiss National Science Foundation (SNF135477) held by WJ Z' Graggen and J. Beck.

Acknowledgements

We thank the members of the Departments of Neurology and Neuroradiology for their support in this study and also our graphic illustrator Anja Giger.

Declaration of conflicting interests

The author(s) declared the following potential conflicts of interest with respect to the research, authorship, and/or publication of this article: JE has received travel grants from Boehringer Ingelheim, Bayer Vital, Bracco Imaging; honoria for oral presentations from Penumbra Europe, Bracco Imaging; and remuneration for advisory boards by Boehringer Ingelheim.

Authors' contributions

RR, JE, and MFO were responsible for UPI and MRP/CTP data acquisition, analysis and interpretation, drafting the article, and critically revising its intellectual content. RW, JG, and UF were in charge with MRP/CTP data acquisition, analysis and interpretation, comparison between two quantification algorithms in TTP Quantification between UPI and MRP. PYG and SW were responsible for analysis and interpretation of the data, technical assistance in ultrasound, and revising the intellectual content of the manuscript. AR and HPM were responsible for the critical revision of the manuscript and discussions. JE, WJZ, and JB were responsible for conception and designing of the study, ethic commission approval, found raising, data analysis and interpretation, drafting of the article. All authors approved the final version to be published.

References

1. Seidel G, Algermissen C, Christoph A, et al. Harmonic imaging of the human brain: visualisation of brain perfusion with ultrasound. *Stroke* 2000; 31: 151–154.
2. Eyding J, Krogias C, Schöllhammer M, et al. Contrast-enhanced ultrasonic parametric perfusion imaging detects dysfunctional tissue at risk in acute MCA stroke. *J Cereb Blood Flow Metab* 2006; 26: 576–582.
3. Kern R, Diels A, Pettenpohl J, et al. Real-time ultrasound brain perfusion imaging with analysis of microbubble replenishment in acute MCA stroke. *J Cereb Blood Flow Metab* 2011; 31: 1716–1726.
4. Kern R, Perren F, Kreisel S, et al. Multiplanar transcranial ultrasound imaging: standards, landmarks and correlation with magnetic resonance imaging. *Ultrasound Med Biol* 2005; 31: 311–315.
5. Krogias C, Postert T, Meves S, et al. Semiquantitative analysis of ultrasonic perfusion imaging. *Ultrasound Med Biol* 2005; 31: 1007–1012.
6. Federlein J, Postert T, Meves S, et al. Ultrasonic evaluation of pathological brain perfusion in acute stroke using second harmonic imaging. *J Neurol Neurosurg Psychiatry* 2000; 69: 616–622.
7. Cosgrove D and Lassau N. Imaging of perfusion using ultrasound. *Eur J Nucl Med Mol Imaging* 2010; 37: S65–S85.
8. Seidel G, Greis C, Sonne J, et al. Harmonic grey scale imaging of the human brain. *J Neuroimaging* 1999; 9: 171–174.
9. Rim SJ, Leong-Poi H, Lindner JR, et al. Quantification of cerebral perfusion with ''real-time'' contrast-enhanced ultrasound. *Circulation* 2001; 104: 2582–2587.
10. Eyding J, Nolte-Martin A, Krogias C, et al. Changes of contrast-specific ultrasonic cerebral perfusion patterns in the course of stroke; reliability of region-wise and parametric imaging analysis. *Ultrasound Med Biol* 2007; 33: 329–334.
11. Willats L, Connelly A, Christensen S, et al. The role of bolus delay and dispersion in predictor models of stroke. *Stroke* 2012; 43: 1025–1031.
12. Galimanis A, Jung S, Mono M-L, et al. Endovascular therapy of 623 patients with anterior circulation stroke. *Stroke* 2012; 43: 1052–1057.
13. Sobesky J, Weber Zaro O, Lehnhardt F-G, et al. Which time-to-peak threshold best identifies penumbral flow? A comparison of perfusion-weighted magnetic resonance imaging and positron emission tomography in acute ischemic stroke. *Stroke* 2004; 35: 2843–2847.
14. Meyer-Wiethe K, Cangür H, Schindler A, et al. Ultrasound perfusion imaging: determination of thresholds for the identification of critically disturbed perfusion in acute ischemic stroke – a pilot study. *Ultrasound Med Biol* 2007; 33: 851–856.
15. Maciak A, Kier C, Seidel G, et al. Detecting stripe artifacts in ultrasound images. *Digit Imaging* 2009; 22: 548–557.
16. Lindsey BD, Light ED, Nicoletto HA, et al. The ultrasound brain helmet: new transducers and volume registration for in vivo simultaneous multi-transducer 3-D transcranial imaging. *IEEE Trans Ultrason Ferroelectr Freq Control* 2011; 58: 1189–1202.
17. Seidel G, Cangür H, Albers T, et al. Sonographic evaluation of hemorrhagic transformation and arterial recanalization in acute hemispheric ischemic stroke. *Stroke* 2009; 40: 119–123.